A COUPLED CLUSTER STUDY OF VAN DER WAALS INTERACTIONS OF THE He ATOM WITH CN, NO AND O_2 RADICALS

Juraj RAAB[a1], Andrej ANTUŠEK[a2,b], Stanislav BISKUPIČ[c] and Miroslav URBAN[a3,*]

[a] *Department of Physical and Theoretical Chemistry, Faculty of Natural Sciences, Comenius University, SK-842 15 Bratislava, Slovakia; e-mail:* [1] *raab@fns.uniba.sk,* [2] *aantusek@fns.uniba.sk,* [3] *urban@fns.uniba.sk*

[b] *Institute of Inorganic Chemistry, Slovak Academy of Sciences, Dúbravská cesta 9, SK-842 36 Bratislava, Slovakia; e-mail: uachantu@savba.sk*

[c] *Department of Physical Chemistry, Slovak University of Technology, Radlinského 9, SK-812 37 Bratislava, Slovakia; e-mail: biskupic@cvt.stuba.sk*

Received August 25, 2003
Accepted November 8, 2003

Dedicated to Professor Rudolf Zahradník on the occasion of his 75th birthday.

The partially spin-adapted coupled cluster method with the restricted open-shell Hartree–Fock reference was applied to calculations of interaction energies between the helium atom and the three radicals, CN ($^2\Sigma$), NO ($^2\Pi$), and O_2 ($^3\Sigma_g^-$). Basis set dependences with medium-augmented correlation consistent basis sets were alleviated by using extrapolations to the basis set limit which were based on aug-cc-pVTZ and aug-cc-pVQZ results. The two-dimensional potential energy surfaces were fitted by exponential and polynomial functions. Minima and transition states were located. Potential energy surfaces are very floppy, especially for HeCN. This complex exhibits the weakest van der Waals interaction, the electronic interaction energy being 92 μE_h. Interaction energy in HeNO is 122 μE_h, almost the same as was found for HeO_2 (124 μE_h). Considering zero-point-vibrational corrections, the dissociation energy of HeCN, HeNO, and HeO_2 is 4.6, 6.6, and 7.3 cm^{-1}, respectively. This sequence of the magnitude of interaction energies and the structural data for global and local minima and transition states were compared with available literature data. No simple link between the magnitude of intermolecular forces and dipole moments and dipole polarizabilities of CN, NO, and O_2 was found. The low-order long-range model based on the induction and dispersion forces is completely useless in the assessment of the sequence of the size of intermolecular interactions of the HeCN, HeNO, and HeO_2 complexes.

Keywords: Coupled cluster calculations; van der Waals complexes; Interaction energy; Potential energy surface; HeCN; HeNO; HeO_2; *Ab initio* calculations; CCSD(T).

Van der Waals intermolecular interactions between atoms and molecules rank among the weakest interactions studied by chemists. Their tremendous importance in many areas of physics, chemistry, and biology was

stressed and summarized in a comprehensive book and in reviews[1–3]. Interactions of noble gas atoms[4] are examples of very low van der Waals interaction energies. The energy range of this phenomena sets high demands on experimental techniques as well as on the accuracy of *ab initio* methods used for their description.

Van der Waals complexes of the helium atom with small open-shell molecules were studied extensively by both experimental and theoretical chemists. The experimental data are mostly coming from spectroscopic measurements of bound states[5–8] and scattering experiments[9–13].

The *ab initio* interaction energy potential surface for the HeCN complex was published by Werner *et al.*[14] They analyzed the CN ground state ($X^2\Sigma$) and the $A^2\Pi$ excited state surfaces obtained at the MCSCF-CI level from the point of view of intermolecular collisions. Among the experimentalists, Halpern and Huang[15] studied the collisional fluorescence quenching of the $A^2\Pi \rightarrow X^2\Sigma^+$ transfer for the He, Ne, and Ar.

Concerning the HeNO complex, its dissociation energy is known to be a part of an experimental program devoted to the NO complexes with noble gas atoms[16,17]. Experimental results for HeNO were obtained by Howard *et al.*[18] using the radio-frequency and the microwave spectroscopy. The ground state of NO is the $^2\Pi$ state and can be split into two states due to the interaction with the helium atom. Thus, the two states of the HeNO complex may emerge, namely the $^2A'$ and the $^2A''$ state, depending on whether the interacting helium atom approaches NO in the in-plane direction of the open-shell π electron or in the out-of-plane direction. A study of both states was theoretically carried out by Yang and Alexander[19] using the CEPA approximation. Different results, even different energy ordering of the states follows from the MP4/MP2 results of Zolotoukhina and Kotake[17]. More recently, rigorous *ab initio* calculations of the HeNO system were performed by Lee and Wright[20] and by Klos, Chalasiński *et al.*[21]

Most attractive for both experimentalists and theoreticians has been the HeO_2 complex. Early studies of the two-dimensional HeO_2 surface were performed by van Lenthe *et al.*[22] and by Jaquet and Staemmler[23]. A more recent results of Cybulski *et al.*[24] were already in good agreement with the empirical surfaces obtained by Keil *et al.*[25], Faubel *et al.*[26], and Beneventi *et al.*[27] These empirical potentials were obtained by fitting the scattering data[25–27] and also second virial data[27]. Among the most recent works concerning HeO_2, one can mention the cooling in the seeded supersonic expansions of, among others, O_2 in He [28–30] along with the computational studies of this effect[29,30], the three-dimensional *ab initio* potential energy surface by Groenenboom and Struniewicz[31] and the perturbative formula-

tion of dispersion contribution to the interaction energy done by Lukeš *et al.*[32]

An important part contributing to the strength of van der Waals interactions is determined by electric properties of interacting compounds. According to the long-range model, the interaction energy can be decomposed into several terms. The most important attractive terms that determine the longe-range parts of the interaction energy potential surface are induction term and the dispersion term, which both decrease with the intermolecular distance as R^{-6}. The induction term can be physically interpreted as the interaction of the permanent dipole moment with the induced dipole moment of interacting partner compound. The induction (E^{I}) and the dispersion (E^{D}) terms for the case when the polarizability tensor of compound A is isotropic (typically atom), and B is a molecule with a permanent dipole moment μ, are given by the formulae

$$E^{I} = -\frac{1}{2}\alpha_A \mu_B^2 (3\cos^2\theta + 1) R^{-6} \qquad (1)$$

$$E^{D} = -\frac{3}{2}\frac{I_A I_B}{I_A + I_B}[\alpha_A \alpha_B + \frac{1}{3}\alpha_A(\alpha_{\parallel}^B - \alpha_{\perp}^B)(\frac{3}{2}\cos^2\theta - \frac{1}{2})] R^{-6}\,, \qquad (2)$$

where α_A, α_B are mean polarizabilities of the subsystems A and B, respectively, and $\alpha_{\parallel}^B$, $\alpha_{\perp}^B$ are parallel and perpendicular components of the polarizability tensor with respect to the dipole moment direction of compound B. R is the intermolecular distance and θ is the angle between the dipole moment direction and the position vector of interacting compound A. In this formulation are both compounds treated as being composed of point charge distributions, but for large R this is a reasonable approximation[1,33].

Obviously, Eqs (*1*) and (*2*) are the low-order long-range formulae, which are useful at most as a tool for the first estimate of the long-range intermolecular forces. For a closer insight, the more elaborated perturbation theory of intermolecular forces[34,35] is needed. Such analysis has been performed for HeNO [21], HeO_2 [24,32] or for NeCN [36] which is related to our HeCN complex. For obtaining interaction energies of weakly bound complexes, more frequently used is the supermolecular approach. The interaction energy is obtained as a difference between the energy of the complex (the supersystem) and the sum of energies of monomers. A highly sophisticated method capable of recovering the intramolecular and the intermolecular

correlation effects must be used for weak van der Waals intermolecular interactions. A prerequisite is a capability of describing correctly electric properties of the monomers[1]. Highly accurate dipole moments and static dipole polarizabilities of CN, NO, and O_2 radicals were calculated in our previous works[37–39].

The idea of this work is to analyze relative interaction energies of the model systems composed of the helium atom interacting with CN, NO, and O_2 radicals. Their electric properties differ quite significantly and thus it was interesting to show how they affect the potential energy curves in their long-range part and also whether they affect the relative magnitude of the interaction of these radicals with the helium atom around the minima. We want to compare the three systems, HeCN, HeNO, and HeO_2 by using the same basis set and the same method. Calculations published so far and cited above were made by different methods and basis sets which makes detailed comparison of the magnitude of intermolecular forces of the three systems and their physical background difficult. Another aspect of the present work is the stability of results with respect to the basis set, which ranks among the most critical aspects of calculations of weak interactions with most standard methods.

THEORETICAL APPROACH AND COMPUTATIONAL DETAILS

The standard supermolecular approach was used for interaction energy calculations, where the interaction energy is given as

$$E_{\mathrm{int}}^{(1)} = E_{\mathrm{AB}}^{(1)} - E_{\mathrm{A}}^{(1)} - E_{\mathrm{B}}^{(1)} . \qquad (3)$$

E_{AB} is the energy of the supersystem and E_{A} and E_{B} are energies of standalone monomers A and B, respectively. Due to the incompleteness of basis sets, the interaction energy as defined above includes the basis set superposition error (BSSE). The standard approach of eliminating BSSE is the use of the counterpoise correction defined by Boys and Bernardi[40]. Following their prescription, the so called ghost basis set of monomer A (B) is added to basis set of monomer B (A). Energies of the monomers calculated with basis sets extended with these ghost basis functions are used in Eq. (*3*) instead of plain energies E_{A} and E_{B}. The interaction energy is normally reduced when BSSE correction is applied. The size of the basis set superposition error is a parameter detecting completeness of the basis sets used. It is important that basis sets that have BSSE not large in comparison with the plain interaction

energy $E_{\mathrm{int}}^{(1)}$, Eq. (*3*), are used. This is another requirement imposed on the selected basis sets, along with the ability of a correct description of electric properties of the subsystems.

The superscript l in Eq. (*3*) denotes the level of the theory and stands for the SCF or for the selected correlated method, namely CCSD and CCSD(T) [41,42]. CCSD is an iterative procedure for obtaining the single (t_i^a) and double (t_{ij}^{ab}) excitation amplitudes. Triples in CCSD(T) are approximated in a perturbative way by using the converged CC amplitudes. A single determinant reference for CC methods is a restricted open-shell Hartree–Fock wave function. An advantage of using the ROHF reference rather than the conceptually more simple and more straightforward UHF (unrestricted HF) wave function in open-shell systems is its more rigorous physical meaning. Namely, the ROHF wave function is a proper eigenfunction of the spin operators while the UHF reference is not. Another advantage of the ROHF reference is a significantly better efficiency of the subsequent CC code in which one can profit from the fact that the orbital space of the ROHF reference is about half of that in the UHF reference. To preserve the proper spin properties in the CC step, the CC excitation amplitudes must be properly spin-adapted[43–46] even if the reference is a proper eigenfunction of the spin operators. In our implementation, based primarily on the formulation of Paldus *et al.*[46], see also ref.[47], we do it only partially, like in an equivalent approach of Knowles, Hampel and Werner[44]. A more rigorous spin-adapted CC method was defined and implemented by Szalay and Gauss[45]. An efficient and still sufficiently accurate implementation of the partially spin-adapted CCSD approach is represented by the algorithm in which only dominating double excitation t_{ij}^{ab} cluster amplitudes are adapted (the DDVV approximation[48]). This version of the ROHF-CCSD was used in this work, followed by non-iterative triples to obtain the CCSD(T) energy. All calculations were carried out by the MOLCAS program package[49].

Standard aug-cc-pVTZ and aug-cc-pVQZ basis sets were used for interaction energy calculations[50,51]. Augmented basis functions in these basis sets are essential for proper description of the diffuse part of the electron distribution needed for correct calculations of atomic and molecular static electric properties[52]. They are also unavoidable in weak van der Waals interactions[53]. Dipole moments and dipole polarizabilities of interacting radicals treated in this paper were sufficiently accurate[37–39] when basis sets of this type were used within the partially spin-adapted ROHF CCSD(T). After extrapolation to the complete basis set limit (CBS limit), these data may serve as benchmark results[39] for electric properties of these radicals.

RESULTS AND DISCUSSION

Two-dimensional potential energy surfaces of He···AB were computed. Numerical results for all three complexes correspond to the spherical coordinate system (R,θ,ϕ), where R is the distance between the He atom and geometrical center of the radical, θ is the angle between the He atom and the positive part of the z-axis. The polar angle ϕ is kept zero. The geometrical center of the radical was identical with the origin of the coordinate system and the symmetry axis of the radical was identical with the z-axis. Interatomic distances R_{AB} of the CN, NO, and O_2 radicals were fixed at their experimental values[54] 1.1718, 1.1530, and 1.20752 Å, respectively. Radical geometries were defined as follows: CN (z(N) = 0.5859 Å, z(C) = –0.5859 Å), NO (z(N) = 0.5765 Å; z(O) = –0.5765 Å), and O_2 (z(O1) = 0.60376 Å, z(O2) = –0.60376 Å).

Most of the calculated data used in the numerical fitting of the potential energy surface (see the next subsection) were obtained with the reasonably extended aug-cc-pVTZ basis set. This basis is found to be the smallest basis set capable of providing reasonable results for, *e.g.*, HeNO [20]. Additional calculations in the vicinity of the minima were obtained with the larger aug-cc-pVQZ. The reduced number of points at the energy surface with the larger basis set allows geometry optimization with slightly lower accuracy but yet accurate enough for interaction energy considerations and for the assessment of the basis set effects. BSSE-corrected interaction energies are presented in Table I and compared with the selected literature data. The ROHF, CCSD, and CCSD(T) potential energy curves with the aug-cc-pVTZ basis are visualized in Figs 1, 2, and 3, respectively, for HeCN, HeNO, and HeO_2. The angle θ for each complex in these figures was kept near its optimal CCSD(T) value to allow a simple view of interaction curves in our three systems.

Basis Set Effects in the Optimized T-Shape Minima and Linear Structures

The first insight into the strength of the interaction in the three systems is provided by CCSD(T) results with the aug-cc-pVTZ basis set. The weakest interaction energy at this level is found for HeCN with the interaction energy $E_{int}^{(CCSD(T))}$ = 82.6 μE_h. Interaction energies for HeNO and HeO_2 are significantly larger. For HeNO and HeO_2 we found the $E_{int}^{(CCSD(T))}$ 111.9 and 107.1 μE_h, respectively. Potential energy curves have no minima at the SCF level except a shallow long-range minimum of HeCN near 5 Å. The interaction of these systems is thus a purely electron correlation effect detected

primarily by CCSD, with triples in CCSD(T) contributing by about 10–20% to the total interaction energy.

The aug-cc-pVTZ basis set yields larger basis set superposition errors than are interaction energies itself, see Table I. With the aug-cc-pVQZ basis is

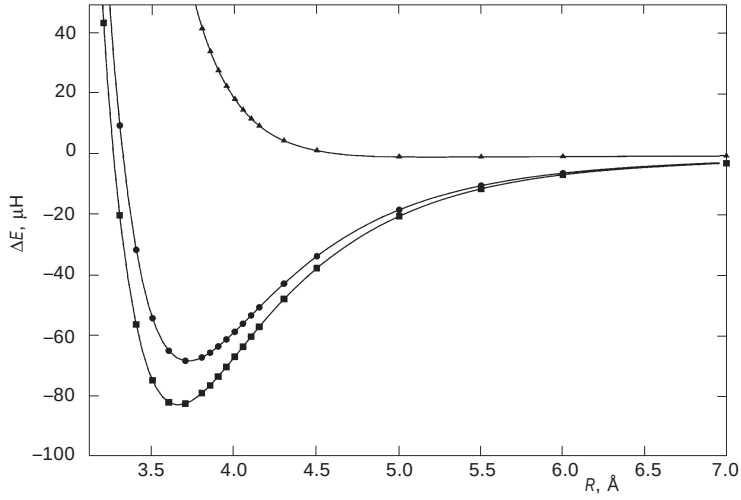

FIG. 1
HeCN BSSE-corrected CCSD(T) interaction energies for θ = 63°. ▲ ROHF, ● ROHF/SA CCSD, ■ ROHF/SA CCSD(T)

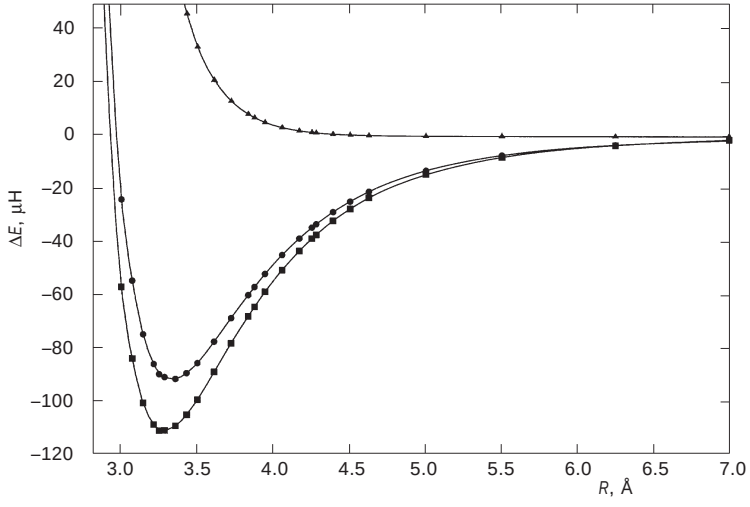

FIG. 2
HeNO BSSE-corrected CCSD(T) interaction energies for θ = 100°. ▲ ROHF, ● ROHF/SA CCSD, ■ ROHF/SA CCSD(T)

BSSE reduced by an order of magnitude in some cases, although it still remains quite high. An alternative technique to treat the problem of the basis set deficiencies in intermolecular interactions is based on the use of the bond-centered basis functions[55] (b.f.) that extend the routinely available basis sets, like aug-cc-pVTZ. Their use improves the convergence to the complete basis set (CBS) limit significantly, but it defines additional parameters that need to be considered, such as a point at which additional basis functions should be centered. Also the extrapolation to the CBS limit would appear to be less systematic, at least for interactions which involve atoms and molecules. In simpler systems like He–He, is the extrapolation technique with bond-centered basis functions highly successful[56]. A comparison of our results with those obtained with basis sets supplemented by bond-centered functions for individual interacting complexes will be presented later.

Instead of using bond-centered functions, we rather rely on available extrapolation techniques using the two relatively satisfactory basis sets, namely aug-cc-pVTZ and aug-cc-pVQZ. It would be tedious to go beyond the aug-cc-pVQZ basis set for a sufficiently large portion of the energy hypersurface. Extrapolations to the CBS limit[57,58] proved to be a very useful tool in various applications, including molecular electric properties[39] and intermolecular interactions[58,59,60]. The most frequently used is a linear extrapolation with respect to the inverse cube of the cardinal number X in

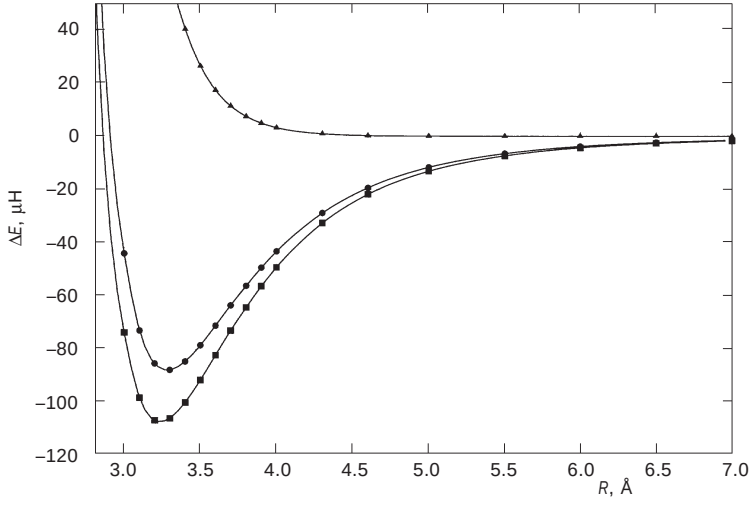

FIG. 3

HeO_2 BSSE-corrected CCSD(T) interaction energies for θ = 90°. ▲ ROHF, ● ROHF/SA CCSD, ■ ROHF/SA CCSD(T)

TABLE I

BSSE-corrected CCSD(T) interaction energies of HeCN, HeNO, and HeO_2 for selected geometries. CBS extrapolation is based on aug-cc-pVTZ and aug-cc-pVQZ basis sets. Our data are compared with the best data available from the literature

System	Basis set	R, Å	θ, °	E_{int}, μE_h	BSSE, μE_h
HeCN	aug-cc-pVTZ	4.01	0.0	–79.23	458.14
HeCN	aug-cc-pVQZ	3.99	0.0	–84.87	45.18
HeCN	CBS	3.98	0.0	–88.99	–
HeCN	aug-cc-pVTZ	3.65	63.0	–82.56	–
HeCN	aug-cc-pVQZ	3.61	66.0	–89.45	–
HeCN	CBS	3.58	68.2	–94.48	–
HeCN	aug-cc-pVTZ	4.09	180.0	–70.03	404.45
HeCN	aug-cc-pVQZ	4.06	180.0	–74.39	44.87
HeCN	CBS	4.04	180.0	–77.57	–
HeNO	aug-cc-pVTZ	3.93	0.0	–77.89	199.27
HeNO	aug-cc-pVQZ	3.92	0.0	–83.60	51.51
HeNO	CBS	3.90	0.0	–87.77	–
HeNO [21]	aug-cc-pVTZ + b.f.	3.93	0.0	–87.90	–
HeNO	aug-cc-pVTZ	3.72	180.0	–92.95	304.68
HeNO	aug-cc-pVQZ	3.68	180.0	–99.70	48.34
HeNO	CBS	3.64	180.0	–104.63	–
HeNO [21]	aug-cc-pVTZ + b.f.	3.66	180.0	–104.34	–
HeNO	aug-cc-pVTZ	3.27	A′ 97.5	–111.88	–
HeNO	aug-cc-pVQZ	3.22	A′ 98.8	–117.77	–
HeNO	CBS	3.18	A′ 99.7	–122.06	–
HeNO [21]	aug-cc-pVTZ + b.f.	3.21	A′ 96.7	–133.04	–
HeNO [20]	aug-cc-pVTZ	3.35	A′ 80.1	–106.97	–
HeNO	aug-cc-pVTZ	3.23	A″ 90.0	–88.453	–
HeNO [21]	aug-cc-pVTZ + b.f.	3.32	A″ 76.1	–115.28	–
HeNO [20]	aug-cc-pVTZ	3.28	A″ 79.9	–85.20	–
HeO_2	aug-cc-pVTZ	3.70	0.0	–101.15	201.37
HeO_2	aug-cc-pVQZ	3.67	0.0	–108.66	53.52
HeO_2	CBS	3.65	0.0	–114.14	–
HeO_2 [31]	aug-cc-pVTZ + b.f.	3.65	0.0	–116.70	–
HeO_2	aug-cc-pVTZ	3.24	90.0	–107.12	60.22
HeO_2	aug-cc-pVQZ	3.20	90.0	–116.95	38.31
HeO_2	CBS	3.17	90.0	–124.12	–
HeO_2 [31]	aug-cc-pVTZ + b.f.	3.17	90.0	–127.10	–

the series of cc-pVXZ basis sets[57]. Quite efficient and generally applicable is also a fit with respect to the inverse number of basis functions in a systematically extended series of basis sets[39,58].

Interaction energies at the CBS limit, as presented in Table I, agree very well with published data for linear structures of HeNO and HeO_2 complexes. The same holds for the geometry parameters. No data using analogous methods and basis sets for the HeCN complex are available in the literature. Linear structures of the two states of HeNO and the HeO_2 complexes are just local minima, for HeCN it is a transition state. Clearly, the interaction energy for linear structures is the strongest for HeO_2. Our CBS values for both linear structures of HeNO and for the HeO_2 complex differ from the published data obtained with CCSD(T) and aug-cc-pVTZ + b.f. basis sets by 2.6 μE_h (0.6 cm^{-1}) or less[21,24,31]. Our results show that the difference between the two basis sets, aug-cc-pVTZ and aug-cc-pVQZ are larger for HeO_2 than for HeCN and HeNO. Consequently, the CBS limit differs from the directly calculated result for HeO_2 more than for the two remaining complexes.

Concerning bent structures, which are absolute minima for all complexes, it is clear that HeCN remains the least stable complex. It is less stable than HeNO and HeO_2 by about 30 μE_h (6.6 cm^{-1}) with all basis sets and at the CBS limit. The agreement between our results and published CCSD(T) results[21,31] with the aug-cc-pVTZ + b.f. basis set for the bent structures of HeNO and HeO_2 is less accurate than for linear structures. Namely, relative stabilities of HeNO and HeO_2 from our results and from results with aug-cc-pVTZ + b.f. basis sets differ. CCSD(T) with aug-cc-pVTZ + b.f. basis sets results indicate that the bent structure of the A′ HeNO is by 6 μE_h more stable than HeO_2. Our CBS-extrapolated results indicate that the stability of both complexes is about the same, HeO_2 being more stable than A′ HeNO by negligible 2 μE_h (less than 0.5 cm^{-1}). Directly calculated CCSD(T) values with the aug-cc-pVQZ basis set show even less different stabilities of the two complexes, supporting, however, larger stability of HeNO this time, as was the case with the aug-cc-pVTZ basis set. The change of the sequence of the stability of HeNO and HeO_2 with the CBS-extrapolated data results, again, from larger sensitivity of the interaction energy to basis sets for HeO_2 than for HeNO. This holds at all geometries. Thus, E_{int} of HeO_2 is affected by the extrapolation to the CBS limit more than the interaction energy of HeNO. Differences between results with the larger aug-cc-pVQZ basis set and the CBS limits are quite systematic, which gives some confidence to our final results. The problem with comparisons of stabilities is that even if

both HeNO [21] and HeO_2 [31] use CCSD(T) and quite similar (but not identical) aug-cc-pVTZ + b.f. basis sets, the calculations did not follow entirely the same routes. A tiny difference in creating bond functions is encountered in calculations for both complexes. Along with differences in basis sets, results may also be affected by using slightly different geometry optimization strategies. Very floppy energy hypersurfaces prevent accurate optimizations. Our results can be affected by the limited number of points calculated in the aug-cc-pVQZ basis set. It is clear that HeCN remains the least stable complex (less stable than HeNO and HeO_2 by about 30 μE_h (6.6 cm^{-1}) with all basis sets and at the CBS limit).

We note, finally, that our interaction energy for the T-shaped optimal structure of HeNO agrees excellently with E_{int} = 123.1 μE_h of Lee and Wright[20] who used the aug-cc-pVQZ basis for energy calculation and the aug-cc-pVTZ optimized geometry. We note, however, that their CCSD(T) calculations follow from the unrestricted HF reference and have different diffuse functions on He from those used by us. At both linear geometries, the agreement between our and Lee and Wright[20] results was less accurate but still satisfactory considering differences in the reference and the flatness of the hypersurface, which leads to some uncertainty in optimized geometries. Their best interaction energies, 80 μE_h for $\theta = 0°$ and 93 μE_h for $\theta = 180°$ are close to our aug-cc-pVQZ values, 84 and 100 μE_h, respectively. Even more relevant is quite good agreement between our CBS extrapolated results and aug-cc-pVTZ + b.f. calculations of Klos, Chalasiński *et al.*[21] especially for linear geometries.

Analytical Form of the Potential Energy Surfaces

BSSE-corrected interaction energies (in μE_h) obtained for the series of geometries at the CCSD(T) level with the aug-cc-pVTZ basis set were used for fitting the analytical potential energy surface (PES) of the form

$$E_{int}^{CCSD(T)} = \sum_{L=0}^{6} P_L^0(\cos(n\theta)) \sum_{k=0}^{4} a_k^L [\exp(-b_1(R-b_2))]^k \,, \qquad (4)$$

where the exponential functions are used for fitting the radial part of the potential and associated Legendre polynomials $P_L^0(\cos(n\theta))$ were used for the description of the angular dependence of the potential. The factor n depends on the system. We used n = 1 for fitting HeCN and HeNO data in which the angle θ lies in the interval 0–180°; n = 2 is used for HeO_2 data

with θ varying between 0 and 90°. *R* has values between 2.8 and 7.0 Å. Points with CCSD(T) interaction energies higher than +10 μE_h were excluded from the fitting procedure to guarantee better description of minima and long-range regions. Altogether, we considered 180, 173, and 77 points for HeCN, HeNO (A′ state), and HeO_2, respectively. No additional points generated by the interpolation were needed for fitting procedures. The RMS error was 0.099, 0.148 and 0.423 μE_h for HeCN, HeNO (A′ state) and HeO_2, respectively. All optimized parameters are presented in Tables II–IV. Minima and transition states that follow from the analysis of the analytical PESs are presented in Table V. All analytical PESs provide good description of *ab*

TABLE II
Fitting parameters of the PES for the HeCN system (*a* parameters are in $E_h \times 10^{-6}$, b_1 = 0.8728828 $Å^{-1}$, b_2 = 6.82109561 Å)

L	a_0^L	a_1^L	a_2^L	a_3^L	a_4^L
0	–0.0760231	–2.7160813	–0.2604274	–0.0299956	0.0025405
1	0.0998241	–0.1132750	0.0788458	–0.0080603	0.0000429
2	–0.4359435	–0.4126404	–0.1366918	–0.0281098	0.0030534
3	–0.0007692	0.0617792	–0.0110042	–0.0018728	0.0000630
4	0.0300868	0.0375656	–0.0071034	–0.0054208	0.0007637
5	0.0095914	–0.1804167	0.0635529	–0.0061172	0.0001501
6	0.1090346	–0.1259522	0.0241507	–0.0019434	0.0001138

TABLE III
Fitting parameters of the PES for the HeNO system (*a* parameters are in $E_h \times 10^{-6}$, b_1 = 0.986162181 $Å^{-1}$, b_2 =3.81746751 Å)

L	a_0^L	a_1^L	a_2^L	a_3^L	a_4^L
0	0.1862261	–39.1971390	–49.8317978	–8.3247488	37.6038506
1	0.0559062	–2.4431399	–17.4059274	24.4138448	12.2357865
2	0.0373799	–10.6104128	–18.8467825	–25.8898341	57.8540349
3	–0.0917286	0.2836150	1.7338588	–14.8984797	7.7667302
4	–0.1371992	–1.2267360	11.1951992	–41.8242663	11.6704022
5	–0.0827914	1.9116386	–5.6354483	1.8288363	–0.9423430
6	–0.2999121	2.4421956	–3.4879946	–4.1060717	0.8144566

TABLE IV
Fitting parameters of the PES for the HeO_2 system (a parameters are in $E_h \times 10^{-6}$, b_1 = 1.34549202 $Å^{-1}$, b_2 = 3.80448160 Å)

L	a_0^L	a_1^L	a_2^L	a_3^L	a_4^L
0	–1.1826052	–77.1444263	–14.8182597	11.9128311	7.2578282
1	–0.7544552	–5.7672131	–53.5988810	51.6159883	–6.2580883
2	–0.1107221	–4.4675158	3.1790539	–12.0705174	5.0073488
3	0.0996326	–4.0543043	5.9253488	–7.6097606	3.2665685
4	–0.2922018	3.8066551	–25.5053983	28.4913520	–8.2923654
5	0.2918023	–3.6688998	19.3183005	–20.9355541	5.4096163
6	–0.0450041	9.2489363	–7.2543190	2.8846134	–1.2869635

TABLE V
Stationary points of PESs for the ground states of HeCN, $^2A'$ HeNO, and HeO_2

Stationary point[a]	R, Å	θ, °	E_{int}, μE_h	ΔE_{int}, μE_h (cm^{-1})[b]
		HeCN PES		
T1	4.0106	0.00	–79.17	3.32 (0.7)
M	3.6461	64.87	–82.49	0
T2	4.0948	180.00	–70.07	12.42 (2.7)
		$^2A'$ HeNO PES		
M1	3.9395	0.00	–77.79	34.09 (7.5)
T1	4.0087	51.38	–44.52	67.36 (14.8)
M2	3.2697	97.48	–111.88	0
T2	3.7458	136.41	–64.98	46.89 (10.3)
M3	3.7293	180.00	–92.93	18.95 (4.2)
		HeO_2 PES		
M1	3.6946	0.00	–101.09	6.04 (1.3)
T	3.6285	51.83	–73.57	33.54 (7.4)
M2	3.2339	90.00	–107.13	0

[a] M, minimum; T, transition state. [b] Relative to the absolute minimum.

initio data. This is demonstrated by rather small differences between PESs and *ab initio* points which are below 0.5% for all significant points. The PESs for HeCN, HeNO, and HeO_2 are visualized in Figs 4–6. The basis set effects on the relative positions of the T-shaped minima with respect to the linear conformations of all complexes were analysed in the previous subsection. We note that the maximum deviations between the values presented in Table V and the CBS limit values for HeCN, HeNO, and HeO_2 were 2.3, 1.4, and 4.0 μE_h, respectively, *i.e.* always less than 1 cm^{-1}. The similarity of

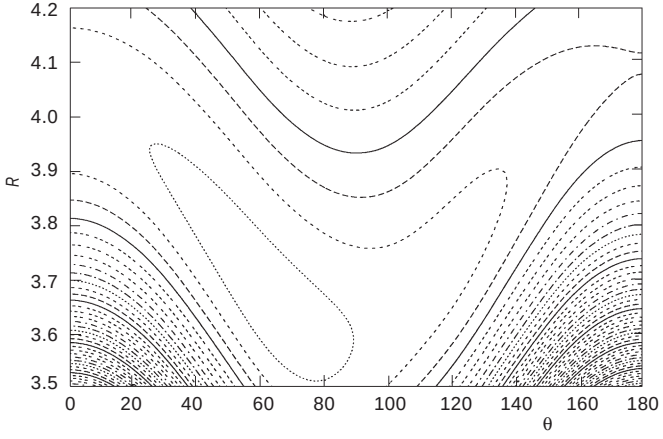

FIG. 4
HeCN CCSD(T) contour plot. The contour lines are separated by 10 μE_h

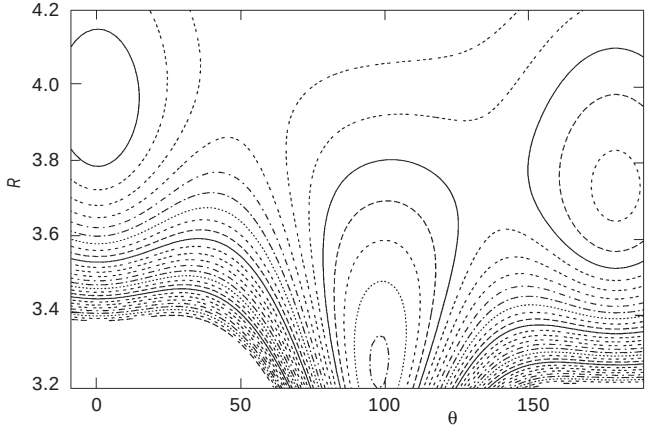

FIG. 5
A′ HeNO CCSD(T) contour plot. The contour lines are separated by 10 μE_h

the basis set effects in the part of the PES at which important points are located gives us some idea about the accuracy of barriers to which we will refer below.

The HeCN Complex

The potential energy surface for HeCN (Fig. 4) is simple, revealing only one T-shaped minimum, as is the case with NeCN, see ref.[36] It is located at the nitrogen side, with θ = 64.9° (Table V). We note that with the enlargement of the basis set the angle θ slightly rises. Both linear structures, with He on the nitrogen side or on the carbon side, are transition states, which separate this minimum from the equivalent minimum localized symmetrically with respect to the CN bond axis. The barrier height is only 3 μE_h on the nitrogen side (θ = 0°) and about 12 μE_h on the carbon side (θ = 180°) of the surface. The HeCN PES is almost isotropic and flat. This isotropy explains why the difference between *ab initio* minima and PES minima is about 2° (Tables I and V), which is considered to be large taking into account the high accuracy of the fit.

The $^2A'$ HeNO Complex

Since a detailed discussion on the relative stability of the A′ and A″ states of HeNO has been published recently (see refs[20,21] and references therein), we will pay attention to the more stable A′ state only. The A′ HeNO PES accom-

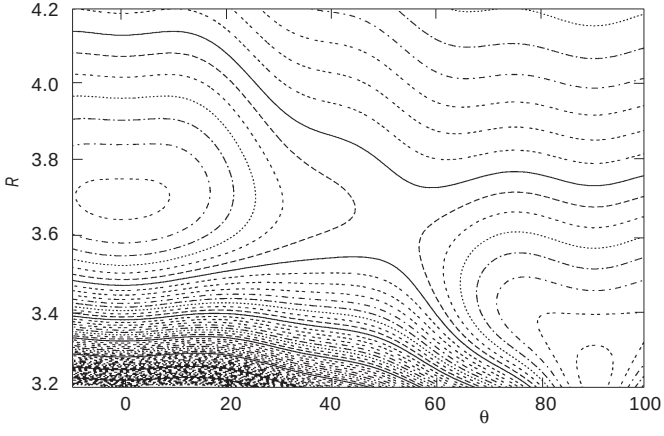

FIG. 6
HeO_2 CCSD(T) contour plot. The contour lines are separated by 5 μE_h

modates three minima (see Table V). The global T-shaped minimum is localized at θ = 97.5°. The barrier, 67 μE_h (14.8 cm^{-1}) high, separates the global minimum from the linear local minimum at θ = 0° (nitrogen side). The barrier between the global minimum and the second minimum that corresponds to the linear geometry with θ = 180° (oxygen side) is 47 μE_h (10.3 cm^{-1}). It agrees well with the barrier calculated by Lee and Wright[20] (9.3 cm^{-1}). Their barrier on the nitrogen side, however, is reported to be much lower than ours, only 6.5 cm^{-1}. We have no reasonable explanation of this discrepancy in light of the fact that other characteristics of the PES agree very well.

The HeO_2 Complex

The HeO_2 PES has two minima. The barrier, which separates the global minimum represented by the T-shaped structure (θ = 90°) from the local minimum, and which corresponds to the linear configuration, is about 34 μE_h high (the same as that reported by Cybulski *et al.*[24]). The saddle point is located at θ = 51.8°. Groenenboom and Struniewicz[31] obtained with the aug-cc-pVTZ basis supplemented by bond functions quite a similar angular location of the barrier (θ = 49°) as well as its height (36.8 μE_h). The barrier for the movement of the He atom from its linear position to the T-shaped structure is 27.5 μE_h high.

The Long-Range Interaction Model

In this part we pay attention to the long-range region of PESs, where induction and dispersion terms dominate. Figure 7 shows the angular dependence of the CCSD(T) interaction energy for all systems and comparisons with the dominating lowest-order long-range terms, $E^I + E^D$, as calculated from Eqs (*1*) and (*2*). The cross-section over PESs corresponds to one selected distance between He and the bond center of the radical, R = 7.0 Å, the same for all complexes. This distance is supposed to be large enough to allow a comparison of the long-range $E^I + E^D$ terms and CCSD(T) interaction energies calculated with the aug-cc-pVTZ basis set. At larger R, interaction energies are too small to guarantee sufficient accuracy needed for comparisons. Long-range terms are based on atomic and molecular properties collected in Table VI.

General features of the angular dependence of *ab initio* data and the dependence that follows from the leading induction and dispersion terms are similar. Linear structures of all complexes (including HeCN) are minima, as

it follows from other studies of the long-range forces and perturbative analyses for systems under study[24]. Although $E^I + E^D$ interaction energies are systematically less attractive than are *ab initio* data for all three systems, the sequence of the interaction strength following from *ab initio* data and long-range contributions remains the same over the large portion of the surface. Slightly different is the shape of the two curves for HeO_2 at angles around $\theta = 90°$. We attribute a flat shape of the CCSD(T) curve around $\theta = 90°$ and the existence of the two maxima at $\theta = 65$ and $115°$ to the

TABLE VI
Ionization potentials (I_p), dipole moments (μ), and static dipole polarizabilities (α) for He, CN, NO, and O_2 from CCSD(T) aug-cc-pVTZ calculations (see also refs[38,39]). All values are in a.u.

System	I_p	μ	$\alpha_{\parallel}$	$\alpha_{\perp}$	$\langle\alpha\rangle$
He	0.902	–	1.38	1.38	1.38
CN	0.505	0.550	25.41	16.19	19.27
NO	0.353	0.066	15.03	9.12	11.35
O_2	0.461	0.000	15.01	8.02	10.35

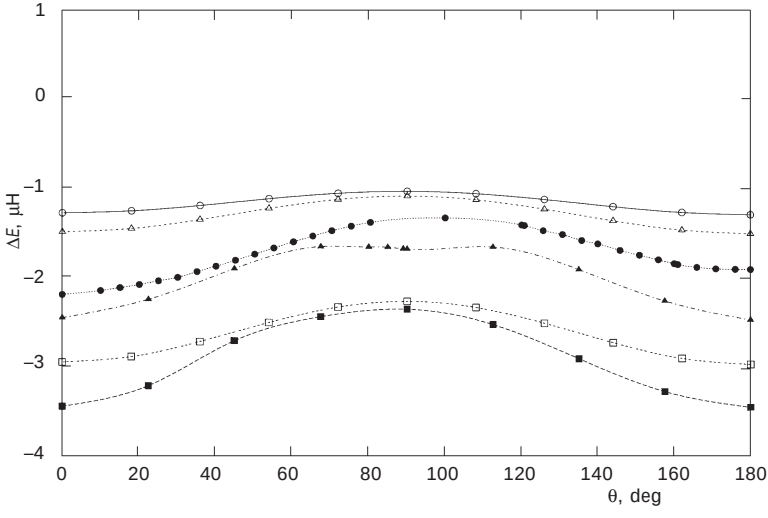

FIG. 7
CCSD(T) interaction energy compared with the $E^I + E^D$ interaction energy at $R = 7.0$ Å. ■ CCSD(T) HeCN, ● CCSD(T) HeNO, ▲ CCSD(T) HeO_2, □ $E^I + E^D$ HeCN, ○ $E^I + E^D$ HeNO, △ $E^I + E^D$ HeO_2

residuum of the transition state that separates the two minima with θ = 90 and 0°, respectively.

The most strongly interacting system in the long-range region is HeCN. This clearly follows from the fact that the CN radical has much larger polarizability than NO and O_2. The dispersion term, a pure electron correlation effect, is driven by polarizabilities. Although the CN radical has also a large dipole moment, this fact does not play any important role because the induction term (which depends on the dipole moment) contributes more than twenty times less than the dispersion term. The induction term plays a role at the SCF level. This explains a shallow long-range SCF minimum about at R = 5 Å on the potential energy curve for HeCN, even though it is not visible in Fig. 1. No such minimum is observed for the remaining complexes that have very low (HeNO) or zero (HeO_2) dipole moments. Since the induction contribution is largest at the linear configuration, the strongest interaction energy results from $E^{I} + E^{D}$ for θ = 0 and 180°. The dispersion contribution, Eq. (*2*), has its isotropic and anisotropic part. The isotropic part dominates, but the anisotropic part, which prefers linear structures, is also quite important at angles approaching θ = 0 and 180°, representing about one quarter of the total E^{D}.

Another point that should be mentioned is that the dipole moment of CN is known to be sensitive to the spin contamination of the CCSD wave function[37,39]. The dipole moment of CN, calculated by the CCSD(T) method, in which CCSD amplitudes are not-spin adapted, increases by 0.043 D after considering the spin adaptation. However, due to the small contribution of the induction term, no effect of the spin adaptation is observed. We note that the CCSD(T) polarizability of CN is affected by the spin adaptation much less[38] than the dipole moment. The insensitivity of the CCSD(T) interaction energies to the spin adaptation applies to the whole energy potential surface, not only in the long-range region.

The leading dispersion and induction terms describe qualitative features in the long-range region of the potential energy surface quite well. However, at shorter distances between He and the radical, other physical effects, including higher-order dispersion terms contribute significantly[1,34,35,61,62] and thus the simple long-range model is completely unsatisfactory here. The importance of higher order dispersion terms for HeO_2 was stressed recently[32]. The angular dependence of the repulsive second-order exchange energy in HeNO was analysed in detail by Klos, Chalasiński *et al.*[21] Its behaviour was rationalized by the inspection of the interaction of He with the π* antibonding orbital of NO.

An oversimplified estimate of the order of stabilities in the series HeCN, HeNO, and HeO_2, based on the low-order dispersion and induction terms alone, would lead to the expectation that HeCN is the most stable species. This follows from its largest dipole moment, dipole polarizability and the dipole polarizability anisotropy. In fact, CCSD(T) calculations show that HeCN is the least stable complex. Also, the linear conformations are preferred by the dispersion and induction terms. However, CCSD(T) data show that the global minima of all the three systems have T-shaped configurations. The stability of the three complexes is essentially governed by the behaviour of the electron correlation contribution considered by CCSD(T), which is counterbalanced by the exchange repulsion. Its principal part is included in the SCF part of the interaction energy. One can easily see from Figs 1–3 that even at relatively short selected bond distance of 4 Å is the CCSD(T) electron correlation contribution to the interaction energy much larger in HeCN (–85 μE_h) than in HeNO and HeO_2 (–53 and –52 μE_h, respectively). Around the minima the situation is changed, the electron correlation contributions are –144, –170, and –199 μE_h for HeCN, HeNO, and HeO_2, respectively. Note, that the optimum R for HeCN is about 0.4 Å larger than that of HeNO and HeO_2, as can be expected from the larger van der Waals radius of carbon than of both nitrogen and oxygen elements. The decomposition of the interaction energies around the global minimum based on the symmetry adapted perturbation theory leads to qualitatively similar results (the dispersion energy, $E_{disp}^{2,0}$, is –142, –193, and –193 μE_h for HeCN, HeNO, and HeO_2, respectively). The exchange repulsion for HeCN at the equilibrium geometry is lower than that for HeNO and HeO_2 (the respective values are 97, 145, and 137 μE_h). It is obvious, that for shorter distances between He and CN the exchange repulsion contribution would increase rapidly, making HeCN less stable. More detailed decomposition of the interaction energy in HeO_2 was published by Klos, Chalasiński *et al.*[21]

Vibrational Correction and Stability of the Complexes

Vibrational and rotational analysis for HeCN [14], HeNO [21], and HeO_2 [31] was not the aim of this work. Yet the vibrational stability is very important in these weakly interacting systems. For this purpose, we have used the harmonic approximation for the estimation of zero-point vibrational levels, which are the upper boundary of exact zero-point vibrational levels calculated by exact vibrational analysis of given potentials. The analytical forms of PESs were transformed to the cartesian coordinate system and matrices of second derivatives were calculated for all minima. Then standard GF

analysis was used for calculation of frequencies of vibrational modes, where we used reduced masses μ(HeCN) = 3.4667, μ(HeNO) = 3.5294, μ(HeO_2) = 3.5556 (in atom mass units). We used an approximation where the radicals are treated as a single atom with the appropriate mass. The results of these calculations are collected in Table VII. Since the optimum geometries are linear or have quasi-T-shape, we can make a correspondence between the ω_1 mode and the radial vibration, and between ω_2 and the angular vibration. Using these frequencies, the zero-point energy defined as $(\omega_1 + \omega_2)/2$ was evaluated for every local minimum. It appears that our approximate approach is quite realistic. Jung and Sun[63] used the three-dimensional PES calculated by Groenenboom and Struniewicz[31] in their vibrational structure calculation on HeO_2. Their ZPE is 21.1 cm^{-1}, in good agreement with our value, 20.0 cm^{-1}, as presented in Table VII. When combined with the electronic well depth from ref.[31] (27.9 cm^{-1}), they arrived at the dissociation energy 6.8 cm^{-1}, again in good agreement with our final estimate of D_0 (see Table VII), 7.3 cm^{-1}.

TABLE VII
Vibrational frequencies, zero-point energies, and dissociation energies in harmonic approximation. Optimized geometries and energies (aug-cc-pVTZ basis) from Table V

	ω_1, cm^{-1}	ω_2, cm^{-1}	ZPE, cm^{-1}	ZPE, μE_h	D_0, μE_h	D_0, cm^{-1}
HeCN						
M1	32.24	0.04	16.14	73.54	8.95	1.96
M1 corr.[a]						4.60
HeNO						
M1	32.63	0.11	16.37	74.59	3.20	0.70
M2	40.14	0.26	20.20	92.04	19.84	4.35
M2 corr.[a]						6.59
M3	37.87	0.11	18.99	86.52	6.41	1.41
HeO_2						
M1	39.28	0.30	19.79	90.17	10.92	2.40
M2	39.92	0.05	19.98	91.03	16.10	3.53
M2 corr.[a]						7.26

[a] Considering $E_{int}^{CCSD(T)}$ from the CBS limit (Table I).

ZPE reduces binding energies considerably, but the dissociation energies $D_0 = E_{min}$ + ZPE show (Table VII) that all three complexes may exist. We note, however, that the aug-cc-pVTZ PES can safely accommodate just the lowest vibrational states and thus all complexes may easily dissociate to their components. The hypersurface for HeCN is especially flat. With ZPE this complex is close to a free rotor. Since PESs around important points are not too much basis-set-dependent, we have substituted the aug-cc-pVTZ electronic interaction energies by their CBS limit values and estimated D_0 as the sum of these energies with vibrational corrections from the aug-cc-pVTZ PES. The obtained dissociation energies, 4.6, 6.6, and 7.3 cm^{-1} for HeCN, HeNO, and HeO_2, respectively, are considered as our best estimates of dissociation energies at zero temperature.

CONCLUSIONS

We have compared the CCSD(T) potential energy surfaces and relative stabilities of the three radicals, $^2\Sigma$ CN, $^2\Pi$ NO, and $^3\Sigma$ O_2, with the He atom. In the analytical fit over 180, 173, and 77 points of PESs for HeCN, HeNO, and HeO_2, respectively, we have exploited the exponential functions and associated Legendre polynomials. The minima and transition states were localized and analyzed.

The T-shaped structure is common for the global minima of all complexes. HeNO and HeO_2 complexes have additional minima in their linear conformations. For HeCN the linear conformation represents a transition state between the two equivalent T-shaped minima. All PESs are very flat. The HeCN complex is characterized by almost completely isotropic PES. With ZPE this complex is close to a free rotor. The electronic interaction energy in HeCN is 94.5 μE_h (20.7 cm^{-1}). The barrier to rotation of the He atom is very low, 3.3 μE_h (0.7 cm^{-1}) at the nitrogen side and 12.4 μE_h (2.7 cm^{-1}) on the carbon side. The bonding in HeNO and HeO_2 is significantly stronger than it is in HeCN, even if the difference is somewhat reduced when vibrational corrections are considered. Interaction energies of HeNO and HeO_2 are practically the same as it follows from our most sophisticated CBS limit values, which are based on the extrapolation of interaction energies with the aug-cc-pVTZ and aug-cc-pVQZ basis sets. The electronic interaction energy in the $^2A'$ state of HeNO in its T-shaped structure is 122.1 μE_h (26.8 cm^{-1}). This global minimum is separated from the local linear minima by the barrier 67 μE_h (He on the N-atom side) and the barrier 47 μE_h (He on the O-atom side). The electronic interaction energy of HeO_2 in its T-shaped structure is 124.1 μE_h (27.2 cm^{-1}), practically identical with that for HeNO.

This global minimum is separated from the local linear minima by the barrier 34 μE_h. Thus, the order of stabilities increases from HeCN to HeNO and HeO_2. With the zero-point-vibrational corrections, all three complexes are very weak. D_0 is 4.6, 6.6, and 7.3 cm^{-1}, for HeCN, HeNO, and HeO_2, respectively.

The order of the interaction energies for HeNO and HeO_2 differs from the literature data, which are based on CCSD(T) calculations and aug-cc-pVTZ basis sets supplemented with bond functions. We attribute this discrepancy to the fact that the last two complexes were calculated by different authors who used methods which differ in the detailed construction of bond functions and geometry optimization strategy.

The leading long-range induction and dispersion interactions follow the CCSD(T) data at long distances between He and the interacting radical. For a selected large distance, 7.0 Å, between He and the midpoint of the radical, the strongest interaction is calculated for He interacting with CN. This is related to the fact, that the dipole moment, dipole polarizability and its anisotropy are much higher for CN that for NO or O_2. The dispersion contribution strongly dominates in the long-range forces. At distances around global and local minima, the values of electric properties play no role. Low-order long-range terms are useless even in qualitative estimates of the order of the interaction forces. This is demonstrated by the fact that $E_{int}^{(CCSD(T))}$ is the weakest for HeCN in spite of the fact that the CN radical has a far larger dipole moment than NO and larger polarizability than both NO and O_2.

Support of the Slovak Grant Agency (Contracts No. 1/0115/03 and No. 1/0052/03) is gratefully acknowledged. We thank V. Lukeš for providing the decomposition of the interaction energy. M. Urban has been enjoying the support of Prof. R. Zahradník since the beginning of his scientific carrier. His continuous support, enthusiasm and friendship are greatly acknowledged.

REFERENCES

1. Hobza P., Zahradník R.: *Intermolecular Complexes (The Role of van der Waals Systems in Physical Chemistry and in Biodisciplines)*. Elsevier, Amsterdam 1988.
2. Hobza P., Zahradník R.: *Chem. Rev.* **1988**, *88*, 871.
3. Chalasiński G., Szcześniak M. M.: *Chem. Rev.* **2000**, *100*, 4227.
4. Burda J. V., Zahradník R., Hobza P., Urban M.: *Mol. Phys.* **1996**, *89*, 425.
5. Leopold K. R., Fraser G. T., Novick S. E., Klemperer W.: *Chem. Rev.* **1994**, *94*, 1807.
6. Nesbitt D. J.: *Annu. Rev. Phys. Chem.* **1994**, *45*, 367.
7. Cohen R. C., Saykally R. J.: *J. Phys. Chem.* **1992**, *96*, 1024.
8. Hutson J. M.: *Annu. Rev. Phys. Chem.* **1993**, *41*, 423.

9. Bacic Z., Miller R. E.: *J. Phys. Chem.* **1996**, *100*, 12945.
10. Furio N., Ali A., Dagdigian P. J.: *Chem. Phys. Lett.* **1986**, *125*, 561.
11. Furio N., Ali A., Dagdigian P. J.: *J. Chem. Phys.* **1986**, *85*, 3860.
12. Jihua G., Ali A., Dagdigian P. J.: *J. Chem. Phys.* **1986**, *85*, 7098.
13. Ali A., Jihua G., Dagdigian P. J.: *J. Chem. Phys.* **1987**, *87*, 2045.
14. Werner H. J., Follmeg B., Alexander M. H.: *J. Chem. Phys.* **1988**, *89*, 3139.
15. Halpern J. B., Huong Y., Titauchuk T.: *Astrophys. Space Sci.* **1996**, *236*, 11.
16. Mack P., Dyke J. M., Wright T. G.: *J. Chem. Soc.* **1998**, *94*, 629.
17. Zolotoukhina T. N., Kotake S.: *J. Chem. Phys.* **1993**, *99*, 2855.
18. Mills P. D. A., Western C. M., Howard B. J.: *J. Phys. Chem.* **1986**, *90*, 4961.
19. Yang M., Alexander M. H.: *J. Chem. Phys.* **1995**, *103*, 6973.
20. Lee E. P. F., Wright T. G.: *J. Chem. Phys.* **1998**, *109*, 157.
21. Klos J., Chalasiński G., Berry M. T., Bukowski R., Cybulski S. M.: *J. Chem. Phys.* **2000**, *112*, 2195.
22. van Lenthe J. H., Duijneveldt F. B.: *J. Chem. Phys.* **1984**, *81*, 3168.
23. Jaquet R., Staemmler V.: *J. Chem. Phys.* **1986**, *101*, 243.
24. Cybulski S. M., Burcl R., Szcześniak M. M., Chalasiński G.: *J. Chem. Phys.* **1996**, *104*, 7997.
25. Keil M., Slankas J. T., Kuppermann A.: *J. Chem. Phys.* **1979**, *70*, 541.
26. Faubel M., Kohl K. H., Toennies J. P., Gianturco F. A.: *J. Chem. Phys.* **1983**, *78*, 5629.
27. Beneventi L., Casavecchia P., Pirani F., Vecchiocattivi F., Volpi G. G., Brocks G., van der Avoird A., Heijmen B., Reuss J.: *J. Chem. Phys.* **1991**, *95*, 195.
28. Aquilanti V., Ascenzi D., Cappelletti D., Pirani F.: *Nature (London)* **1994**, *371*, 399.
29. Aquilanti V., Ascenzi D., de Castro Vítores, Pirani F., Cappelletti D.: *J. Chem. Phys.* **1999**, *111*, 2620.
30. Fair J. R., Nesbitt D. J.: *J. Chem. Phys.* **1999**, *111*, 6821.
31. Groenenboom G. C., Struniewicz I. M.: *J. Chem. Phys.* **2000**, *113*, 9562.
32. Lukeš V., Laurinc V., Biskupič S.: *J. Comput. Chem.* **1999**, *20*, 857.
33. Buckingham A. D. in: *Intermolecular Interactions: From Diatomics to Biopolymers* (B. Pullman, Ed.), p. 1. Willey, New York 1978.
34. Chalasiński G., Gutowski M.: *Chem. Rev.* **1988**, *88*, 943.
35. Chalasiński G., Szcześniak M. M.: *Chem. Rev.* **1994**, *94*, 1723.
36. Vrábel I., Lukeš V., Laurinc V., Biskupič S.: *J. Phys. Chem.* **2000**, *104*, 96.
37. Urban M., Neogrády P., Raab J., Diercksen G. H. D.: *Collect. Czech. Chem. Commun.* **1998**, *63*, 1409.
38. Medveď M., Urban M., Kellö V., Diercksen G. H. F.: *J. Mol. Struct. (THEOCHEM)* **2001**, *547*, 219.
39. Neogrády P., Medveď M., Černušák I., Urban M.: *Mol. Phys.* **2002**, *100*, 541.
40. Boys S. F., Bernardi F.: *Mol. Phys.* **1970**, *19*, 553.
41. Raghavachari K., Trucks G. W., Pople J. A., Head-Gordon M.: *Chem. Phys. Lett.* **1985**, *157*, 479.
42. Urban M., Noga J., Cole S. J., Bartlett R. J.: *J. Chem. Phys.* **1985**, *83*, 4041.
43. Neogrády P., Urban M.: *Int. J. Quantum Chem.* **1995**, *55*, 187.
44. Knowles P. J., Hampel C., Werner H.-J.: *J. Chem. Phys.* **1993**, *99*, 5219.
45. Szalay P., Gauss J.: *J. Chem. Phys.* **1997**, *107*, 9028.
46. a) Paldus J.: *J. Chem. Phys.* **1977**, *67*, 303; b) Li X., Paldus J.: *J. Chem. Phys.* **1997**, *102*, 2012.
47. Janssen C. L., Schaefer III H. F.: *Theor. Chim. Acta* **1991**, *79*, 1.

48. Neogrády P., Urban M., Hubač I.: *J. Chem. Phys.* **1994**, *100*, 3706.
49. Andersson K., Barysz M., Bernhardsson A., Blomberg M. R. A., Cooper D. L., Fleig T., Fülscher M. P., de Graaf C., Hess B. A., Karlström G., Lindh R., Malmqvist P.-Å., Neogrády P., Olsen J., Roos B. O., Sadlej A. J., Schütz M., Schimmelpfennig B., Seijo L., Serrano-Andrés L., Siegbahn P. E. M., Stalring J., Thorsteinsson T., Veryazov V., Widmark P.-O.: *MOLCAS*, Version 5. Lund University, Lund 2000.
50. Dunning T. H., Jr.: *J. Chem. Phys.* **1989**, *90*, 1007.
51. a) Woon D. E., Dunning T. H., Jr.: *J. Chem. Phys.* **1994**, *100*, 2975; b) Kendall R. A., Dunning T. H., Jr., Harrison R. J.: *J. Chem. Phys.* **1992**, *96*, 6796.
52. Woon D. E., Dunning T. H., Jr.: *J. Chem. Phys.* **1994**, *100*, 2975.
53. van Mourik T., Dunning T. H., Jr.: *Mol. Phys.* **1999**, *96*, 529.
54. Huber K. P., Herzberg H.: *Molecular Spectra and Structure*, Vol. IV. Van Nostrand Reinhold, New York 1979.
55. Williams H. L., Mas E. M., Szalewicz K., Jeziorski B.: *J. Chem. Phys.* **1995**, *103*, 7374.
56. Jeziorska M., Bukowski R., Cencek W., Jaszunski M., Jeziorski B., Szalewicz K.: *Collect. Czech. Chem. Commun.* **2003**, *68*, 463.
57. Halkier A., Helgaker T., Jorgensen P., Klopper W., Koch H., Olsen J., Wilson A. K.: *Chem. Phys. Lett.* **1998**, *286*, 243.
58. Šroubková L., Zahradník R.: *Helv. Chim. Acta* **2001**, *84*, 1328.
59. Halkier A., Koch H., Jorgensen P., Christiansen O.: *Chem. Phys. Lett.* **1992**, *200*, 113.
60. Alexander M. H.: *J. Chem. Phys.* **1999**, *111*, 7426.
61. Rae A. I. M.: *Mol. Phys.* **1975**, *29*, 467.
62. Jeziorski B., Moszynski R., Szalewicz K.: *Chem. Rev.* **1994**, *94*, 1887.
63. Jung J., Sun H.: *Mol. Phys.* **2001**, *99*, 1867.